Hierarchical Control Strategy of Heat and Power for Zero Energy Buildings including Hybrid Fuel Cell/Photovoltaic Power Sources and Plug-in Electric Vehicle

Ghiasi, Mohammad Iman; Aliakbar Golkar, Masoud ; Hajizadeh, Amin

Published in:
Iranian Journal of Hydrogen and Fuel Cell (IJHFC)

Publication date:
2016

Document Version
Publisher's PDF, also known as Version of record

DOI: http://dx.doi.org/10.22104/ijhfc.2016.312

Iranian Journal of Hydrogen & Fuel Cell 1(2016) 33-44

Iranian Journal of Hydrogen & Fuel Cell

IJHFC

Journal homepage://ijhfc.irost.ir

Hierarchical control strategy of heat and power for zero energy buildings including hybrid fuel cell/photovoltaic power sources and plug-in electric vehicle

Mohamad Iman Ghiasi[1,*] , Masoud Aliakbar Golkar[2], Amin Hajizadeh[3]

[1] Department of Power Electrical Engineering, Science and Research branch, Islamic Azad University, Tehran, Iran.
[2] Department of Electrical and Computer Engineering, K.N.Toosi University of Technology, Teharn, Iran.
[3] Department of Energy Technology, Aalborg University, Denmark.

Article Information

Article History:

Received:
10 June 2016
Received in revised form:
30 June 2016
Accepted:
03 July 2016

Keywords

Adaptive
Fuzzy Control
Hybrid Power Control
Heat
Renewable Energy
Photovoltaic
Fuel Cell
Energy Storage

Abstract

This paper presents a hierarchical control strategy for heat and electric power control of a building integrating hybrid renewable power sources including photovoltaic, fuel cell and battery energy storage with Plug-in Electric Vehicles (PEV) in smart distribution systems. Because of the controllability of fuel cell power, this power sources plays the main role for providing heat and electric power to zero emission buildings. First, the power flow structure between hybrid power resources is described. To do so, all necessary electrical and thermal equations are investigated. Next, due to the many complexities and uncertainties in this kind of hybrid system, a hybrid supervisory control with an adaptive fuzzy sliding power control strategy is proposed to regulate the amount of requested fuel from a fuel cell power source to produce the electrical power and heat. Then, simulation results are used to demonstrate the effectiveness and capability of the proposed control strategy during different operating conditions in the utility grid. Finally, the performance of the proposed controller is verified using hardware-in-the-loop (HIL) real-time simulations carried out in OPAL-RT technologies for a real building in Tehran. The HIL results show that the proposed controller provides the proper power and heat control strategy.

1. Introduction

With more electricity-consuming products coming into our daily lives, such as electrical vehicles (EVs) and advanced heating, ventilation, and air conditioning systems, load demand is increasing dramatically and imposing significant burdens on the existing power grid. The increasing rate for interconnection of distributed power resources and energy storages has created the possibility of microgrid, both in AC and DC forms. Combining both AC and DC systems, hybrid microgrids have been proposed by many researchers [1, 2]. Recently, with additional applications of DC energy storages, plug-in electric vehicles and DC renewable energy sources in residential areas, building integrated-DC power sources have been

*Corresponding E-mail address: m.ghiasi@srbiau.ac.ir

receiving more research attention. Among the DC power resources, fuel cell-based micro-combined heat and power (CHP) systems, in particular, have received increasing attention recently [3-4]. This is due to a number of reasons. First, all somewhat decentralized power sources minimizes distribution power losses. Secondly, a well-developed infrastructure for distributed natural gas is already available in many countries. Therefore, the step to produce electricity in domestic households is realistic if the technical and financial issues of the CHP units can be resolved. For these reasons, the necessity to meet both electrical power and heat management is more challenging for zero emission buildings. Recently, some papers have addressed the issues related to this topic.

In [3], a multi-objective modelling approach that allows optimized design of micro-CHP systems that considers the source, distribution and emissions requirements in unison to achieve more efficient whole systems has been presented. Numerous recent studies [4-5] have focused on building cogeneration applications of polymer electrolyte membrane (PEM) fuel cells (also known as proton exchange membrane fuel cells) because they have high power density (small stack size), high cogeneration efficiency (sum of heat and power), and fast startup time owing to their low operating temperature [4-6]. An effective control strategy is fundamental to exploit all the advantages expected from CHP plants, in particular when innovative technologies, such as fuel cell, are involved [7-8].

Most of papers, have not presented detailed analysis about power electronic converters and power sources. Moreover, the stability analysis and robustness of the proposed controllers has not been discussed during load power changing, charging and discharging of PEV. Therefore, it is necessary to design a power control strategy for building integrated-hybrid DC power sources and flexible loads, in order to mitigate the power intermittency and uncertainty, and provide a stable and reliable power supply for both the utility and local customers. Hence, in this paper a hybrid power flow control structure for building integrated hybrid renewable energy resources and a plug-in electric vehicle is proposed. In order to build the hybrid power sources combined with the plug-in electric vehicle for green buildings in a Simulink environment, mathematical models of photovoltaic, fuel cell, battery, power electronic converters need to be implemented. Furthermore, an adaptive fuzzy sliding power control strategy for managing power between building, photovoltaic, fuel cell power sources and PEV is developed and the zero energy characteristic is investigated. This intelligent control strategy combines an adaptive rule with fuzzy and sliding-mode control technologies. It has an online learning ability for responding to the building load profile's time-varying and the nonlinear uncertainty behaviors of PEV, in addition to adjusting the control rules and parameters. Finally, simulation analyses for different case studies are presented. Moreover, in order to validate the proposed control strategy, it is verified using hardware-in-the-loop (HIL) real-time simulations carried out in OPAL-RT technologies for a real building in Tehran.

2. Proposed system framework

As Fig. 1 shows, the overall system is composed of the utility power grid, the building system, the renewable energy resource and the PEV system. In this paper the renewable energy resources includes photovoltaic and fuel cell which are green energies with zero CO_2 emission. The PEV system could be considered as a new form of distributed mobile energy storage. It is combined with the distributed renewable energy resources and the controllable load (the smart building). Moreover, a battery energy storage is considered in the building to keep the energy balance for the whole hybrid system. It is connected to the DC bus through a bidirectional DC-DC converter. In order to implement the whole hybrid power system model, mathematical models for each power resources have been used [9-10].

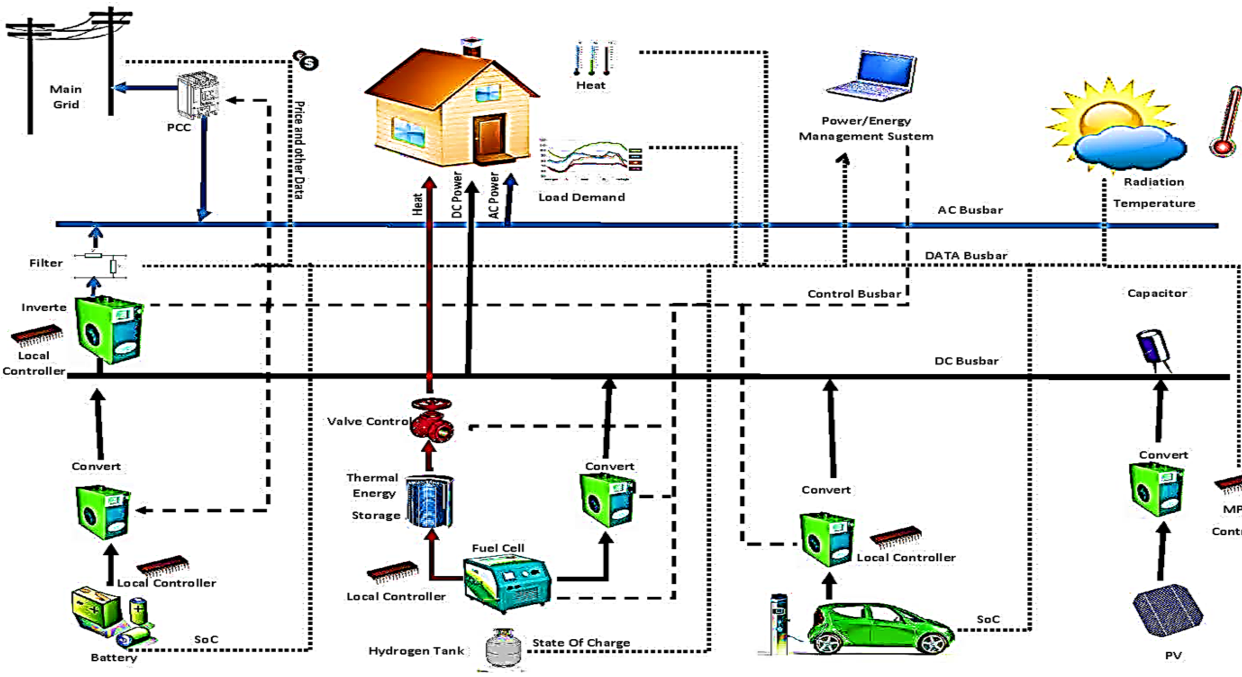

Fig.1. Overall configuration of hybrid renewable power sources combined with a plug-in electric vehicle.

3. Hierarchical control strategy

A common method to control of complex dynamic systems with many uncertainties is designing different local controllers for each specific operating area or determined objects, and then designing a switching strategy through the subsystems to achieve the global objectives of the system.

The control of zero energy building systems involves some complex control processes, such as generating a power command for the fuel cells according to external environment changes and PEV connection expectation, splitting the power between two power-sources to sustain the efficiency of the engine and/or charging/discharging efficiency of the battery at a relatively high level, and supplying the heat and electrical power to meet the requirement from the above battery level. These processes usually involve logic switching, jump, sample-data control signals, and certainly, the continuous signals; hence, the hybrid electric vehicle system is a hybrid dynamical system.

Hybrid and switched systems have numerous applications in the control of mechanical systems, automotive industry, flight and air traffic control, switching power converters, process control, robotics, etc. Hybrid systems consist of a continuous-time and/or discrete-time process interacting with a logical or decision-making process. The continuous/discrete-time subsystem is represented as a set of differential/difference equations whereas the logical/decision making subsystem (supervisor) is represented as a finite state machine or a more general discrete event system, e.g. a Petri net. In the hybrid system context, the continuous/discrete time subsystem affects the discrete transitions of the supervisor and the supervisor affects the dynamic evolution of the continuous/discrete-time subsystem. In this paper, a real-time hierarchical control strategy has been developed for a zero energy building structure. The hierarchical hybrid controller represents a high-level vehicle control system that can coordinate the overall power generation system to satisfy certain operational conditions. This hybrid controller is shown in Fig.2.

According to the proposed controller the battery's state of charge (SOC), PV power (P_{PV}), load power (P_{load}), hydrogen tank pressure (P_{r_H2}), and fuel cell power

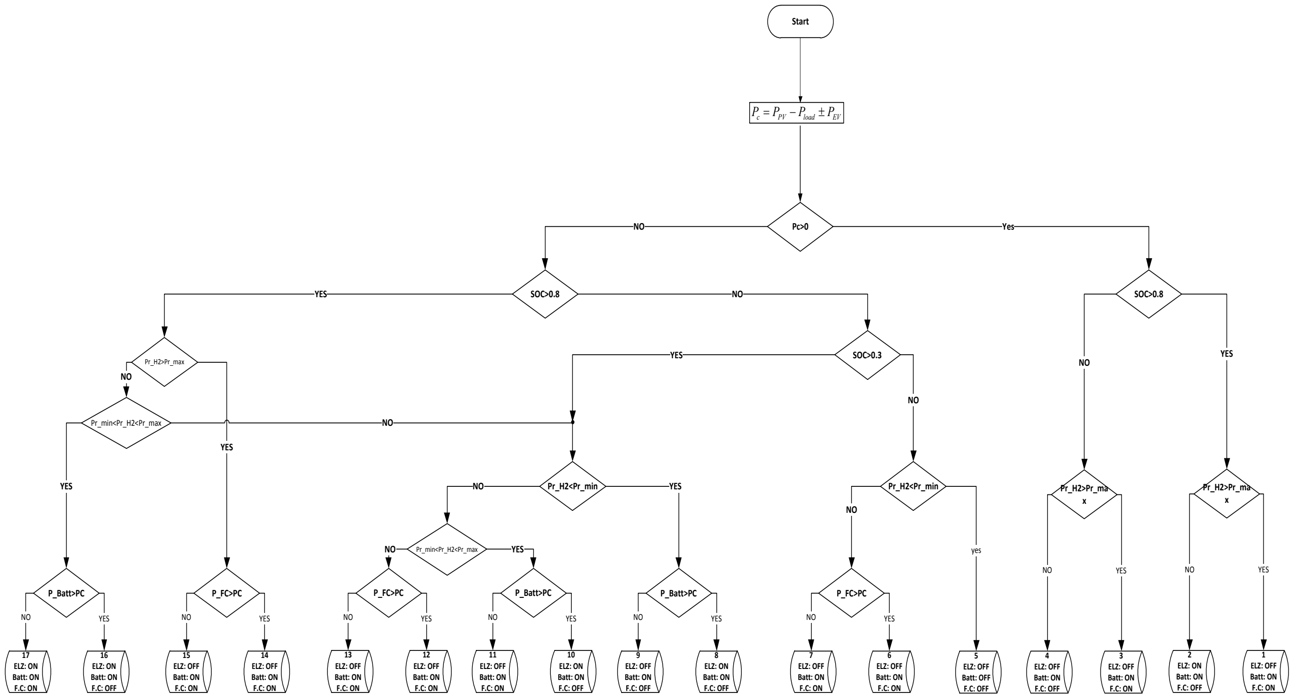

Fig.2. Hybrid control systems for a zero energy building.

(P_{FC}) are considered in the decision making process. Because of the variable structure nature of a hybrid power system for supplying power to a zero energy building, there are 19 possible operating modes. In order to satisfy the electrical and heat power for the building, the supervisory switching strategy decides which operating mode to use according to the structure shown in Fig.2

4. Combined heat and electric power control of fuel cell

Fig.3 shows an overview of the high temperature PEM fuel cell power system for residential applications. Generally, the system consists of a steam reformer, water gas shift reactor, fuel cell heat reservoir, burner and some kind of heat exchanger. The fuel cell itself is placed inside the heat storage reservoir which contains a fluid which remains in liquid form up to 190°C. Hence, all heat released from the fuel cell will be efficiently transferred to the heat reservoir without any losses (electrical or thermal). The advantages of system simplicity are apparent but it puts some challenges on the control system design as the control set points are increasingly coupled [11].

The Nernst's equation and Ohm's law determine the average voltage magnitude of the fuel cell stack. The following equation models the voltage of the fuel cell stack [13]:

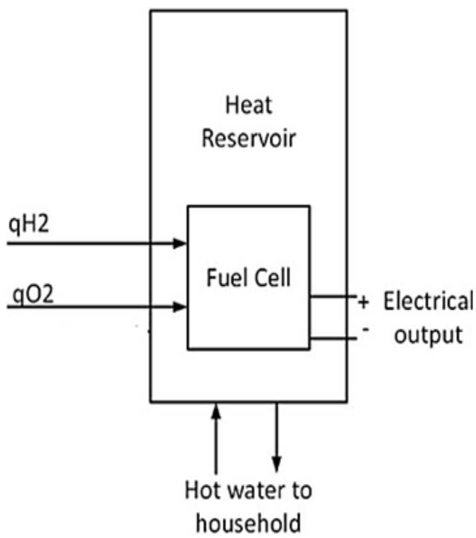

Fig.3. Combined heat and power fuel cell power system.

$$v_{FC} = N_0(E_0 + \frac{RT}{2F}(\ln(\frac{P_{H_2}P_{O_2}^{0.5}}{P_{H_2O}})) - rI_{FC} \quad (1)$$

Where, N_0 is the number of cells connected in series, E_0 is the voltage associated with the reaction free energy, R is the universal gas constant, T is the absolute temperature, i_{FC} is the current of the fuel cell stack, F is the Faraday's constant, and r is the internal resistance of the fuel cell. P_{H2}, P_{H2O}, P_{O2} are hydrogen, water and oxygen pressures which are determined by the following differential equations:

$$\begin{aligned} \frac{dP_{H_2}}{dt} &= -\frac{1}{t_{H_2}}(P_{H_2} + \frac{1}{K_{H_2}}(q_{H_2}^{in} - 2K_r i_{FC})) \\ \frac{dP_{H_2O}}{dt} &= -\frac{1}{t_{H_2O}}(P_{H_2O} + \frac{2}{K_{H_2O}}K_r i_{FC})) \\ \frac{dP_{O_2}}{dt} &= -\frac{1}{t_{O_2}}(P_{O_2} + \frac{1}{K_{O_2}}(q_{O_2}^{in} - K_r i_{FC})) \end{aligned} \quad (2)$$

Where, $q_{H_2}^{in}$ and $q_{O_2}^{in}$ are the molar flow of hydrogen and oxygen and the K_r constant is defined by the relation between the rate of reactant hydrogen and the fuel cell current:

$$q_{H_2}^{r} = \frac{N_0 I_{FC}}{2F} = 2K_r i_{FC} \quad (3)$$

In order to improve the accuracy of the stack model, the dynamic behavior of the cell according to T_{FC} can be derived based on the energy balance principle [11]. The relevant equation is,

$$m_s C_{ps}\frac{dT_{FC}}{dt} = \sum q_{H2}^{in}(\bar{h}_{H2}^{in} - \bar{h}_{H2}^{o}) + \sum q_i^r \bar{h}_{H2}^{o} - P_{FC} \quad (4)$$

where, P_{FC} is the PEMFC DC output power, m_sC_{ps} is the mass-specific heat product of the stack, and h_i is the ith gas per mole enthalpy and it can be written as,

$$\bar{h}_i = \bar{h}_{i,std} + \bar{C}_{pi}.\Delta T \quad (5)$$

In Equation (4), $h_{i,std}$ is the ith gas per mole enthalpy at the standard pressure of 0.1 MPa and the C_{pi} standard temperature T_{std} of 283K, C_{pi} is the ith gas average constant-pressure specific heat, and ΔT is the temperature change. According to equations (2)-(4), all parameters are related to i_{FC} and should be controlled to satisfy both requested fuel cell power and temperature.

The requested temperature (T_{FC_ref}), which is determined based on the requested amount of heat energy, is regulated. Equation (7) shows the relating thermal energy to thermal mass:

$Q=C_{th}\,\Delta T$ where Q is the thermal energy transferred, C_{th} is the thermal mass of the body, and ΔT is the change in temperature.

Proper control of the DC-DC converter is vital to control the fuel cell power (current). Control of the electric power balance from the hybrid renewable power sources and PEV to the smart building and to/from the grid is necessary to maintain power sharing at all times while satisfying the active and reactive power demanded by the home electrical load.

The rate and magnitudes of fuel cell and photovoltaic power P_{FC} and P_{PV} and rate, sign and magnitude of PEV power P_{PEV} depend on the magnitude and how fast the load changes. Here, the PEV power is considered as stochastic energy storage with no control on its power.

$$\begin{aligned} P_{HS} &= P_{FC} + P_{Batt} + P_{PV} \\ P_{Home} &= P_{HS} + P_{Grid} \pm P_{PEV} \end{aligned} \quad (7)$$

According to the control strategy proposed in this paper, P_{Home} is made equal to P_{ref} so that the hybrid power system (HS) output follows the home load demand.

According to equation (7), it is necessary to control the fuel cell power (current) in order to keep the electrical power balance in the DC-link. For this purpose the following equation is considered

$$\begin{aligned} L\frac{di_{FC}}{dt} &= d \times v_{FC} - (1-d) \times v_{dc} \\ C_{dc}v_{dc}\frac{dv_{dc}}{dt} &= P_{Batt} + P_{FC} + P_{PV} - (P_{\mathrm{home}} \pm P_{PEV}) \\ P_{FC} &= i_{FC} \times v_{FC} \end{aligned} \quad (8)$$

By rearranging the above equations, the following standard state space equations are achieved:

$$\dot{X}(t) = f(X(t),u(t),w(t))$$

$$X(\mathrm{t}) = \begin{bmatrix} P_{H_2} \\ P_{H_2O} \\ P_{O_2} \\ T_{FC} \\ V_{dc} \end{bmatrix} \quad (9)$$

$$u = q_{H2}, w(t) = i_{load}$$

Therefore, according to the above equations, *X(t)* is the state vector, *u(t)* is the input vector and *w(t)* is the input disturbance. In the above equation, it is clear that all matrixes and inputs are related to system parameters. As shown, the control input is the amount of hydrogen (q_{H2_ref}) and the input disturbance is the load current (i_{load}) which is composed of the requested current from the building and PEV charging/discharging current. Inherently, equation (9) is nonlinear and time varying. The input disturbance (i_{load}) is unpredictable and has a stochastic nature because of the charging and discharging period of the PEV. Due to the mentioned properties, inaccurate mathematical models, unknown parameters and need for a fast response during power variations, a conventional linear controller could not be used for controlling fuel cell temperature and power. Hence, in this paper an adaptive fuzzy sliding mode control [18] is proposed for controlling the fuel cell. Fuzzy control can provide an appropriate solution for these problems by incorporating linguistic information from human experts as an alternative to conventional control techniques. This approach is gaining increased interests from both the academic world and the industrial field. Despite its practical successes in many areas, fuzzy control seems to be deficient in formal analysis and robustness aspects. On the other hand, the sliding-mode control has been widely employed to control nonlinear systems, especially the systems that have model uncertainty and external disturbance. Robustness is the best advantage of a sliding-mode control. It employs a noncontiguous control effort to drive the system toward a sliding surface, and then switches on that surface. Details of an adaptive fuzzy sliding mode control is introduced in the following section.

5. Adaptive fuzzy sliding mode control

The block diagram of an adaptive fuzzy sliding mode control is shown in Fig. 4. As illustrated, the sliding surface variable (s) is employed as the one dimensional fuzzy input variable.

In order to define the sliding surface, the two following functions are considered:

$$e = \begin{bmatrix} e_1 \\ e_2 \end{bmatrix}$$
$$e_1 = (P_{FC-ref} - P_{FC}) \quad (10)$$
$$e_2 = (T_{FC-ref} - T_{FC})$$

Where *e* is the phase plane variable. Then, the sliding surface on the phase plane can be defined as:

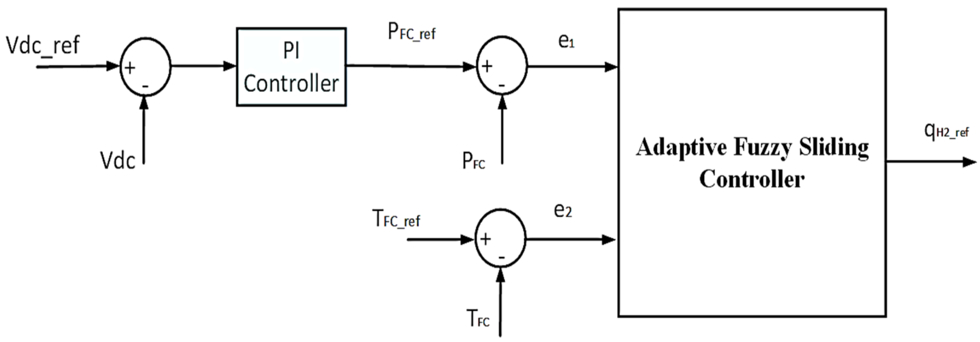

Fig.4. Proposed control structure for Fuel Cell Power Systems.

$$s=\left(\frac{d}{dt}+l\right)e=\frac{d}{dt}\begin{bmatrix}e_1\\e_2\end{bmatrix}+\lambda\begin{bmatrix}e_1\\e_2\end{bmatrix} \tag{11}$$

Based on the Lyapunov theorem, the sliding surface reaching condition is $s.\dot{s}<0$. If a control input *u* can be chosen to satisfy this reaching condition, the control system will converge to the origin of the phase plane. When the condition is s<0, $s.\dot{s}$ will decrease with as u decreases. Based on this qualitative analysis, the control input can be designed in an attempt to satisfy the inequality.

Here, seven fuzzy rules are employed in this control system to obtain the appropriate dynamic response and control accuracy. The input membership functions are scaled into the range of -1 and 1 with an equal span. The control law is derived from the fuzzy inference decision and defuzzification operation.

$$u=\frac{\sum_{l}^{m}\mu^{j}.U^{j}}{\sum_{l}^{m}\mu^{j}}=\frac{\sum_{l}^{m}\mu^{j}.C^{j}}{\sum_{l}^{m}\mu^{j}} \tag{12}$$

Where m is the rules number and C^j is the consequent parameter. Which can be initially set to zero as a zero fuzzy rule beginning. An adaptive rule is used to adjust or update it. The adaptive rule is derived from the steep descent rule to minimize the value with respect to C^j. Then, the modification equation of the parameter is

$$C^{j}=-\eta\frac{\partial s(t).s(t)}{\partial C^{j}(t)} \tag{13}$$

where η is the adaptive rate parameter. Based on the chain rule, the above equation can be rewritten as

$$=-\quad\frac{\partial s(\mathrm{t}).s(\mathrm{t})}{\partial u(\mathrm{t})}\frac{\partial u(\mathrm{t})}{\partial C\ \ (\mathrm{t})}$$

$$=-\quad(\mathrm{t}).\mathrm{s}(\mathrm{t})\frac{\partial\ \ (\mathrm{t})}{\partial\ \ \ (\mathrm{t})} \tag{14}$$

$$(\mathrm{t})\frac{(\mathrm{t})}{\sum\ \ (\mathrm{t})}$$

where the adaptive rate parameter η and the system input parameter *g(t)* are combined as a learning rate parameter θ. Then, the central positions of the defuzzification membership functions can be regulated directly through the modification of consequent parameter, C^j. Hence, it achieves the objectives of online learning and fuzzy rules adjustment.

6. Simulation results

The simulation results were obtained by developing a detailed MATLAB/SIMULINK software package. In order to evaluate the effectiveness of the proposed control strategy, the hybrid power system with all related components was simulated under two different operating conditions of PEV (charging and discharging). The specification of the PV system, the Li-ion battery and PEMFC stack and the power conditioning units' parameters including dc –dc and dc –ac converters are given in Table 1. The performance of the proposed PV/PEMFC/battery hybrid system model was examined under different operating charging and discharging conditions of PEV and simulation results were obtained for the time interval between 0 and 350 s. Moreover, the performance of the proposed controller was verified using hardware-in-the-loop (HIL) real-time simulations carried out in OPAL-RT technologies for a real building in Tehran, as shown in Fig.5. The power demand profile has a significant effect on the performance of proposed control strategy. A practical load profile for two family members in a resident application in TEHRAN city is established through real measuring, as shown in Fig. 6. In order to simulate the PV model, the output power of a real solar power system, which has been installed for the considered building in TEHRAN, is shown in Fig. 7. The output power of the power conditioning unit is the maximum power of PV for each sampling time. From this load profile, it is evident that the average power demand is 6 kW. However, because of weather conditions, the output power of the PV system varies from 0 to 2.8 kW. Also, requested heat power profile for resident application in TEHRAN is illustrated in

Fig.8.

Table 1. Parameters of the Hybrid Power System

Fuel Cell System Parameters	
Nominal Power	25 [kW]
Faraday's constant (*F*)	96484600[C/kmol]
Hydrogen time constant (t_{H2})	26.1 [s]
Hydrogen valve molar constant(K_{H2})	8.43×10^{-4}
kr Constant=N_0/4F	9.9497×10^{-7}
No Load Voltage (E_0)	0.6 [V]
Number of Cells (N_0)	384
Oxygen time constant (t_{O2})	2.91[s]
Oxygen valve molar constant (K_{O2})	2.52×10^{-3}
FC internal resistance (r)	0.126 [Ω]
FC absolute temperature (T)	343 [K]
Universal gas constant (R)	8314.47 [J/(kmol K)]
Utilization Factor (U_f)	0.8
Water time constant (t_{H2O})	78.3 [s]
Water valve molar constant (K_{H2O})	2.81×10^{-4}
Photovoltaic Parameters	
Nominal Power	3[kWp]
Series resistance (R_s)	0.0042 [Ω]
Parallel resistance (R_p)	10.1 [Ω]
Boost DC-DC Converter Parameters	
Rated voltage (V)	200V/650V
Rated power	15 kW
Nominal duty cycle	0.6
Resistance (R)	2.3 [Ω]
Capacitance (C)	1.5 [mF]
Inductor (L)	415 [ηH]
Battery Energy Storage Parameters	
Nominal terminal voltage	48 [V]
Maximum Capacity (Ah)	40[Ah]
Initial State-Of-Charge (%)	65%
DC/AC Converter Parameters	
Nominal AC Voltage	220[V]
Nominal phase current	125 [A]
Nominal DC voltage	100 [V]
R	0.9 [mΩ]
L	0.01[mH]
f_s	50 [Hz]
Controller Parameters	
λ	0.25
m	49

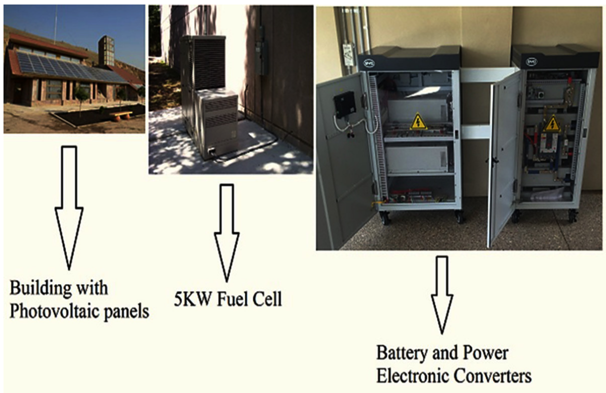

Fig.5. Zero energy building in Tehran.

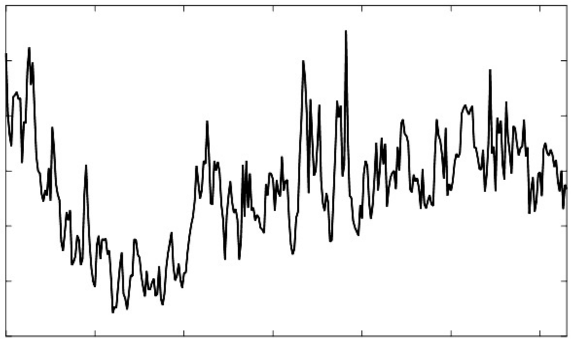

Fig.6. Load active power for resident application in TEHRAN.

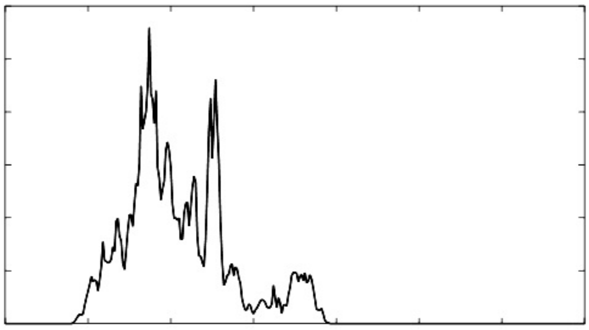

Fig.7. Output power of solar system in TEHRAN.

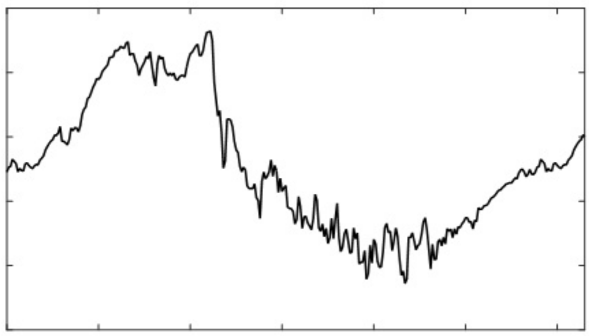

Fig.8. Requested heat power for resident application in TEHRAN.

6.1. Evaluation of proposed control strategy during charging of PEV (Building to Vehicle)

For a residential building with solar panels, fuel cell, and energy storage the impact of PEV charging on the performance of the proposed advanced controller depends on the capacity of the PEV battery, PV, fuel cell and energy storage. The battery energy storage in the building can be used to partially or fully charge the PEV battery to reduce the peak load due to PEV battery charging. In this case study, it is supposed that the PEV is connected to the building for charging of the batteries. Moreover, it is assumed that the PEV charger operates very fast so that 2 KW could be absorbed from the PEV during 100-200 sec. For this purpose, a simulation based on the requested load power (Fig.6) was performed. In Fig. 9 variations of fuel cell voltage and current are presented. As shown, the fuel cell current changes according to the load profile, PV output power and PEV charging profile. It is clear that when the PV is supplying the power the fuel cell current is decreasing, and when the PEV is charging the fuel cell current is increasing.
According to the proposed control strategy, the fuel cell power varies based on the requested electrical and heat power. In Fig.10, the electrical output power and achieved heat power of the fuel cell are shown. It is evident that the output heat power of the fuel cell is bigger than the output electric power of the fuel cell.
The electrical power of the fuel cell is determined based on the proposed adaptive robust controller, which supplies part of the requested active power. In addition, as shown in Fig.10, there is a difference between achieved and requested heat power from the fuel cell. In fact, it depends on the dynamic performance of the fuel cell which is related to the thermochemical equations and time constants of the fuel process.
The hydrogen and airflow rates (liter per minutes) for the fuel cell stack are illustrated in Fig.11. They are regulated based on the total amount of requested power from the fuel cell.
In Fig.12, the battery voltage, battery current and SOC are shown can be seen from the figure, during the charging operation of the PEV, the battery is used to manage the power of the green building. battery could keep the balance between the requested power from the building and the produced power from the fuel cell and PV. Moreover, according to the charging mode of the PEV, battery plays a good role during the charging mode to deliver enough charge power to the PEV. As shown, after charging the PEV the residential battery energy storage goes toward storing the extra power produced by the PV and fuel cell.

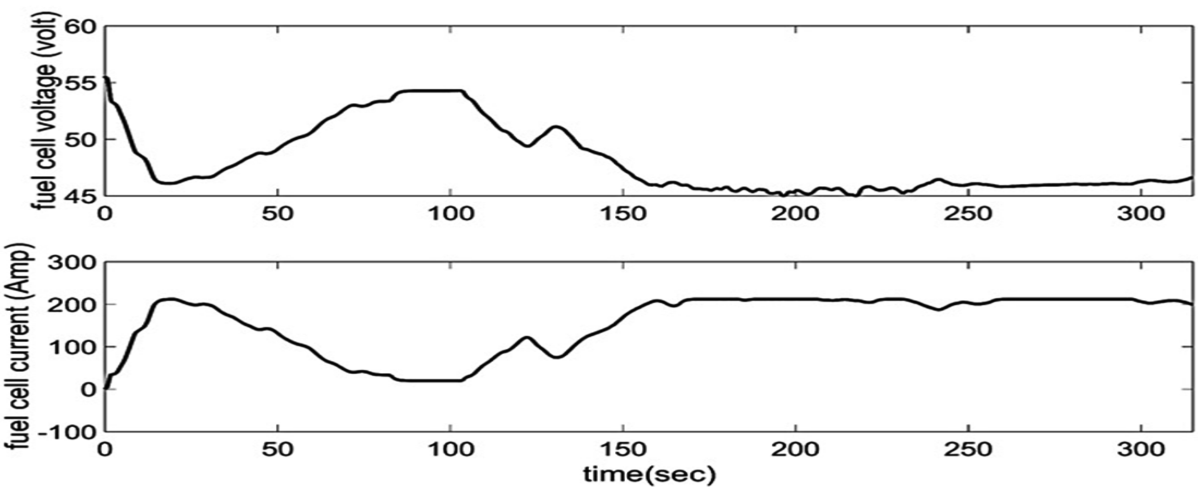

Fig. 9. Variations of fuel cell voltage and current during PEV charging.

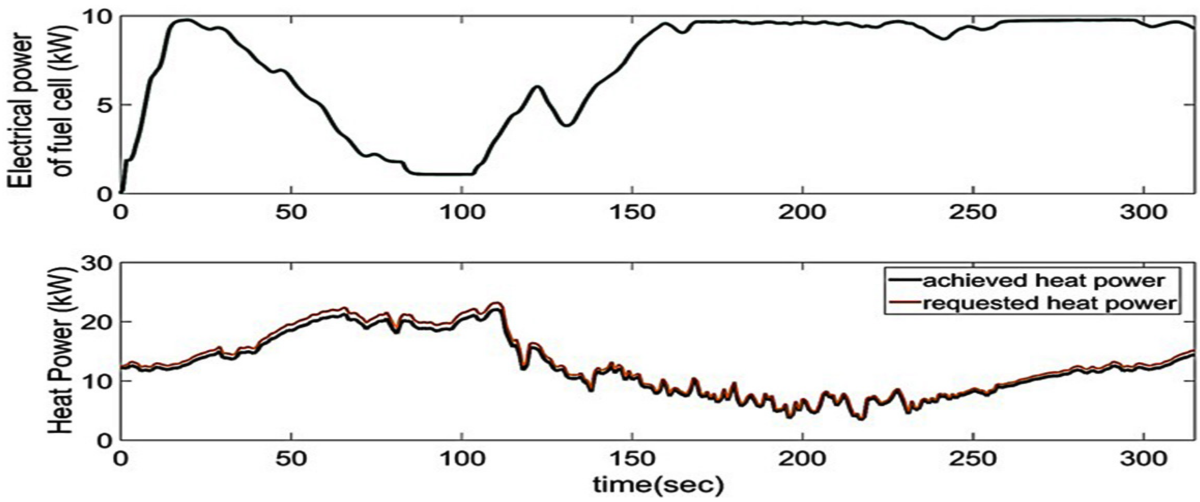

Fig.10. Electrical output power and heat power of the fuel cell during PEV charging.

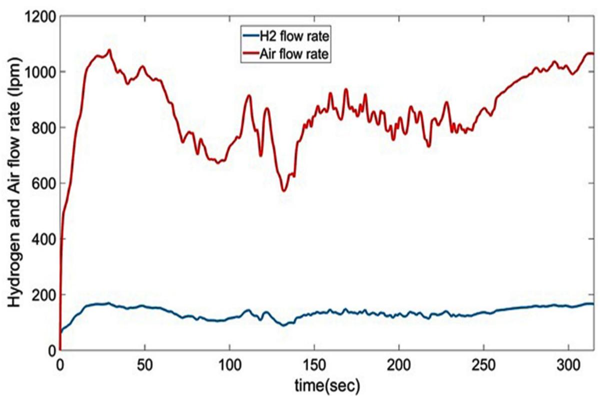

Fig.11. H_2 and air flow rate of fuel cell (lpm) during charging operation of PEV.

5.2. Evaluation of proposed control strategy during discharging of PEV (Vehicle to Building)

Vehicle-to-building (V2B) provides an option to use the battery energy in electric vehicles to support loads in residential buildings. In this case, it is considered that the local demand side management strategy (DSM) is a smart grid. So, it determines the proper time for PEV connection to shift the peak power from the fuel cell as a main energy resource. Therefore, according to the requested load profile from the building, the PEV is integrated with the building between 150-200 sec and delivers power around 2.5kW. Consequently, the dynamic performance of the whole system and the capability of the proposed

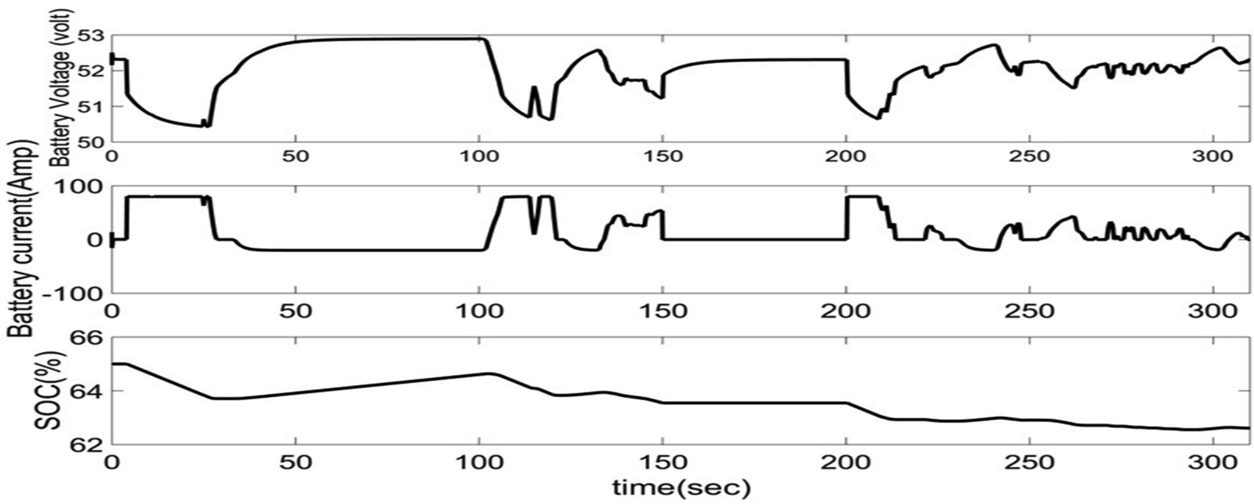

Fig.12. Battery voltage, battery current and SOC during PEV charging.

control strategy are investigated. The variations of fuel cell current and voltage are presented in Fig.13. As illustrated, during PEV discharging (blue box), the fuel cell current reduces and the PEV plays a dynamic reconfigurable energy storage role. The heat power of the fuel cell satisfies the requested heat power from the building completely. In Fig.14, the battery voltage, battery current and SOC are presented. During the PEV discharging condition, the residential battery energy storage is used to store part of the energy and operates under low delivered power to the building. As shown in Fig.14, during PEV discharging operation condition, the battery voltage changes smoothly and the battery's SOC is constant. As mentioned before, the analysis of this paper was investigated dynamically. Therefore, in a dynamic operation point of view, the proposed controller appropriately utilized each part of the power generation system. In general, this analysis could be expanded for the daily operation of a zero emission building and will be considered for future work.

The hydrogen and airflow rates (liter per minutes) for the fuel cell stack during PEV discharging are shown in Fig.15. In this period (blue box) the amount of fuel consumption of fuel cell decreases.

7. Conclusion

In this paper a hierarchical control strategy for a building integrated hybrid renewable power and Plug-in Electric Vehicles in smart distribution systems is investigated. Due to the controllability of fuel cell power, it plays the main role in providing heat and electric power to zero emission buildings. Therefore,

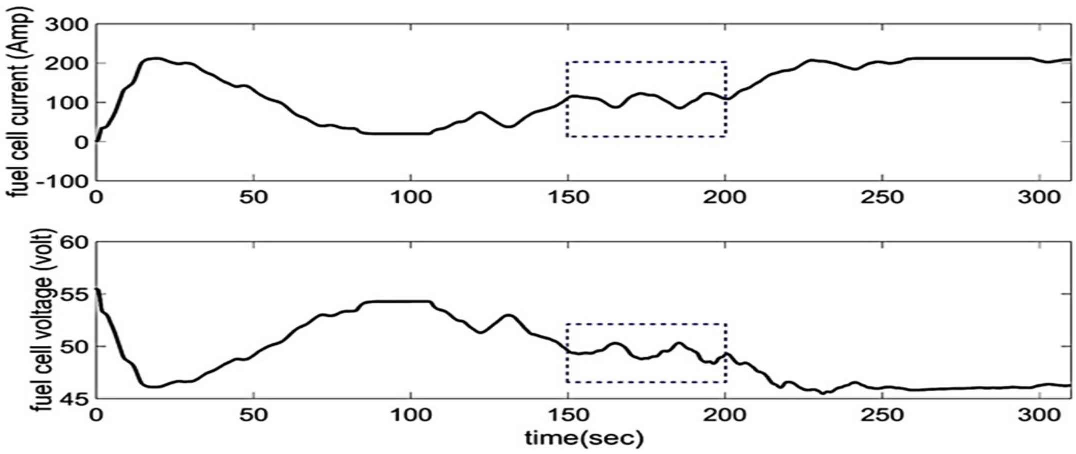

Fig.14. Battery voltage, battery current and SOC during PEV charging.

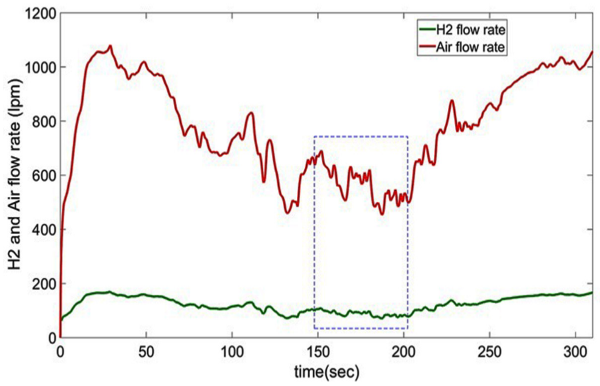

Fig.15. H_2 and air flow rate of the fuel cell (lpm) during the PEV charging operation.

first the hybrid power flow structure between hybrid power resources is described. For this purpose, all necessary electrical and thermal equations are investigated. Then, an adaptive fuzzy sliding power control strategy is proposed to regulate the amount of requested fuel for a fuel cell power source to produce the electrical and heat power. Simulation results are illustrated to demonstrate the effectiveness and capability of the proposed control strategy during different operating conditions in a utility grid. Finally, the performance of the proposed controller is verified using hardware-in-the-loop (HIL) real-time simulations carried out in OPAL-RT technologies for a real building in Tehran. The HIL results show that the proposed controller provides the proper power and heat control strategy.

8. References

[1] H. Kakigano, Y. Miura, and T. Ise. “Configuration and control of a DC microgrid for residential houses,” in Proc. Transmiss. Distrib. Conf. Expo. Asia Pac., Seoul, Korea, pp. 1–4, 2009.

[2] J. J. Justo, F. Mwasilu, J. Lee, and J.-W. Jung “AC-microgrids versus DC-microgrids with distributed energy resources: A review,” Renew.Sustain. Energy Rev., vol. 24, pp. 387–405, 2013.

[3] X. Guan, Z. Xu, and Q.-S. Jia, “Energy-efficient buildings facilitated by microgrid,” IEEE Trans. Smart Grid, vol. 1, no. 3, pp. 243–252, Dec. 2010.

[4] T. Elmer, M. Worall, S. Wu, S.B. Riffat, Fuel cell technology for domestic built environment applications: state of-the-art review, Renew. Sustain. Energy Rev. 42, 913–931, 2015.

[5] H.G.Nguyen, A.Mohamad Aris, B.Shabani, “PEM fuel cell heat recovery for preheating inlet air in standalone solar-hydrogen systems for telecommunication applications: An exergy analysis”, International journal of hydrogen energy 41, 2987-3003, 2016.

[6] A. Adam, E.S. Fraga, D.J.L. Brett, Options for residential building services design using fuel cell based micro-CHP and the potential for heat integration, Appl. Energy 138, 685–694, 2014.

[7] S. Murugann, B.Horák, “A review of micro combined heat and power systems for residential applications”, Renewable and Sustainable Energy Reviews 64, 144–162, 2016.

[8] Colella WG. Design considerations for effective control of an afterburner subsystem in a combined heat and power (CHP) fuel cell system (FCS). J Power Sources 2003; 118:118–28.

[9] A.Hajizadeh, M.Aliakbar Golkar, “Intelligent Robust Control of Hybrid Distributed Generation System under Voltage Sag”, Journal of Expert Systems with Applications, 37, 7627–7638, 2013.

[10] A.Hajizadeh, M.Aliakbar Golkar, “Optimal Intelligent Control of Plug-in Fuel Cell Electric Vehicles in Smart Electric Grids”, Iranian Journal of Hydrogen & Fuel Cell, 1, 55-63, 2014.

[11] B.Najafi, A.Haghighat Mamaghani, F.Rinaldi, A.Casalegno, “Fuel partialization and power/heat shifting strategies applied to a 30 kWel high temperature PEM fuel cell based residential micro cogeneration plant”, International Journal of Hydrogen Energy 40 (2015) 14224-14234.

[12] T. Orowska-Kowalska, M. Kaminski and K. Szabat "Implementation of a sliding-mode controller with an integral function and fuzzy gain value for the electrical drive with an elastic joint", IEEE Trans. Ind. Electron., vol. 57, no. 4, pp.1309 -1317, 2010.

[13] Rong-Jong "Fuzzy sliding-mode control using adaptive tuning technique", IEEE Trans. Ind. Electron., vol. 54, no. 1, pp.586 -594, 2007.